

Different-Guided-Mode-Coupling DBR for WDM Optical Interconnection Board Using Channel Waveguides

Kenji Kintaka (1), Junji Nishii (1), Satoshi Yamaguchi (2), Takayuki Kobayashi (2) and Shogo Ura (2)

1) National Institute of Advanced Industrial Science and Technology, Osaka 563-8577 JAPAN, kintaka.kenji@aist.go.jp

2) Kyoto Institute of Technology, Kyoto 606-8585 JAPAN, ura@kit.ac.jp

Abstract: A distributed Bragg reflector (DBR) coupling TE_0 and TE_1 guided modes was designed and fabricated for constructing an intra-board chip-to-chip optical interconnection with wavelength-division multiplexing. Coupling efficiency of 97% and wavelength selectivity of 2 nm were predicted for interaction length of 0.3 mm. Preliminary experimental results were also reported.

Introduction

Intra-board chip-to-chip optical interconnection is one of strong candidates for solving the so-called pin-bottleneck problem in constructing future ultra-high-speed signal-processing units [1]. Recently, optical interconnect configurations using multimode waveguides as optical signal paths have been investigated extensively because of their high compatibility with printed circuit boards and large fabrication tolerance with low insertion loss [2-7]. As another approach, optical interconnect configurations using free space as optical signal path have been proposed and demonstrated in order to realize two-dimensional (2-D) parallel transmission of optical signals from a 2-D array of vertical cavity surface emitting lasers (VCSELs) to a 2-D array of photodiodes (PDs) so far [8-12]. Most of these techniques have utilized micro-optic components such as micro-mirrors and micro-prisms.

On the other hand, we have proposed and investigated an integrated-optic configuration using a thin-film waveguide as optical signal paths [13-20]. The integrated-optic configuration utilizes wavelength-division multiplexing (WDM) technique with free-space-wave add-drop multiplexers consisting of focusing grating couplers (FGCs) and distributed Bragg reflectors (DBRs). The proposed configuration has advantage in compatibility with printed circuit boards, compactness, and 2-D parallel signal transmission. However, the width of each guided wave should be determined by waveguide length, namely, signal

transmission length, due to diffraction. Therefore, wiring density is limited down to several channels per millimeter for 10-mm transmission length.

In order to improve the wiring density, we have proposed and investigated a new integrated-optic configuration using channel waveguides [21, 22]. The proposed interconnection device consists of vertically Y-branched mode splitters/combiners and different-guided-mode-coupling (DGM) DBRs which couple fundamental and 1st-order modes contra-directionally in order to realize wavelength add-drop multiplexing. The new configuration can have higher wiring density and larger tolerances in input coupling than our previous configuration. In this paper, we report design, fabrication and characterization of a proto-type 2-D DGM-DBR for the first time.

Configuration of intra-board optical interconnection

Cross-sectional configuration of a single waveguide channel of the proposed optical interconnection is illustrated in Fig. 1. Only two WDM signal channels are shown for simplicity. Optoelectronic interposers integrating VCSELs or PDs are surface-mounted with LSI chips on a board. The optical interconnect device in the board consists of two vertically stacked waveguides with different refractive indices. Add/drop and transmission cores are contacted in multiplexing region, while they are separated by a splitting layer in input/output region. The multiplexing and input/output regions are connected with vertical Y-branch region. Both waveguides can guide only fundamental mode in the input/output region. Fundamental TE -like mode of signal transmission waveguide (E_{00}^T mode) in input/output region is coupled to fundamental TE -like (E_{00}^M) mode in the multiplexing region, and fundamental TE -like mode of add/drop waveguide ($E_{00}^{A/D}$ mode) in input/output region is coupled to 1st-order TE -like (E_{01}^M) mode in the multiplexing region. DGM-DBRs are integrated

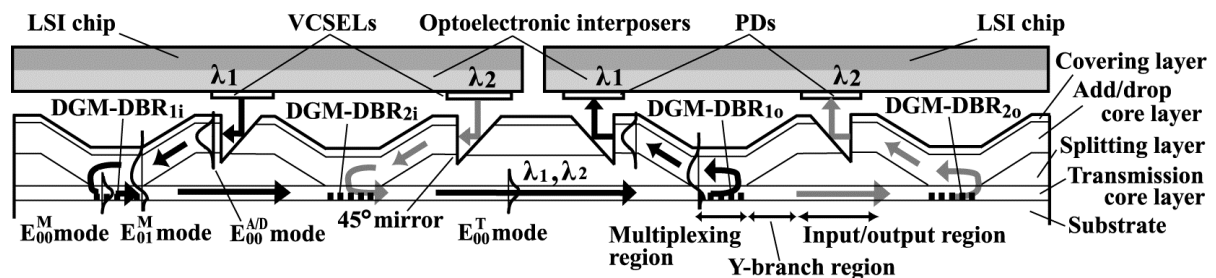


Fig. 1: Schematic view of the optical interconnect configuration

for contra-directionally coupling of E_{00}^M and E_{01}^M modes in the multiplexing region. 45° mirrors are integrated in the input/output regions for input/output coupling of free-space and $E_{00}^{A/D}$ guided waves.

A free-space wave of wavelength λ_1 from a VCSEL is coupled to $E_{00}^{A/D}$ mode by a 45° mirror. The $E_{00}^{A/D}$ mode passes through an add/drop waveguide and an upper branch in Y-branch, and becomes E_{01}^M mode in the multiplexing region. The E_{01}^M mode is contra-directionally coupled to E_{00}^M mode by DGM-DBR_{1i}. The E_{00}^M mode propagates in a lower branch in Y-branch and signal transmission waveguide as E_{00}^T mode, and passes through DGM-DBR_{2i}. The propagated E_{00}^T mode becomes E_{00}^M mode, and is contra-directionally coupled to E_{01}^M mode by DGM-DBR_{1o}. The E_{01}^M mode passes through an upper branch in Y branch and propagates in an add/drop waveguide as $E_{00}^{A/D}$ mode. The $E_{00}^{A/D}$ mode is coupled out to a free-space wave, and reflected to a PD by a 45° mirror. In the same way, a free-space wave of wavelength λ_2 from another VCSEL is transmitted and detected by another PD.

Design of 2-D DGM-DBR

We designed a 2-D DGM-DBR at operating wavelength of 850-nm band. Figure 2 illustrates a cross-sectional structure and a refractive index profile of the designed 2-D waveguide. The thickness and refractive index of add/drop core layer were set to 4 μm and 1.47, respectively, so that the guided-mode profile coincides to beam profile from a single-mode VCSEL. The thickness and refractive index of transmission core layer were set to 0.8 μm and 1.54, respectively. DBR grating was formed by patterning Si-N layer of refractive index of 2.01 and embedded in the bottom of the transmission core layer. The thickness and refractive index of covering layer were set to 1 μm and 1.46, respectively.

The device characteristics were calculated by conventional coupled-mode analysis. Calculated mode profiles of TE_0^M and TE_1^M modes are also shown in Fig. 2. A coupling coefficient of DGM-DBR between TE_0^M and TE_1^M modes was calculated to be 8.3 mm^{-1} with grating groove depth of 0.03 μm . Figure 3 shows the calculated wavelength dependence of cou-

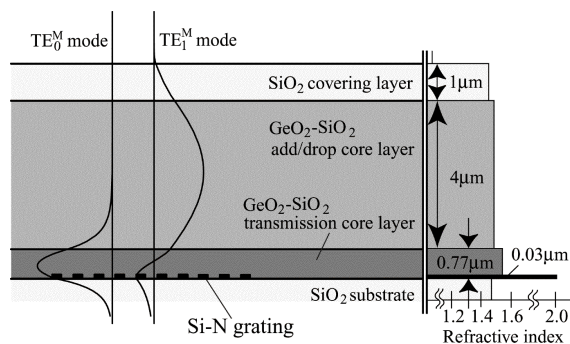


Fig. 2: Cross-sectional structure and refractive index profile of the designed DGM-DBR

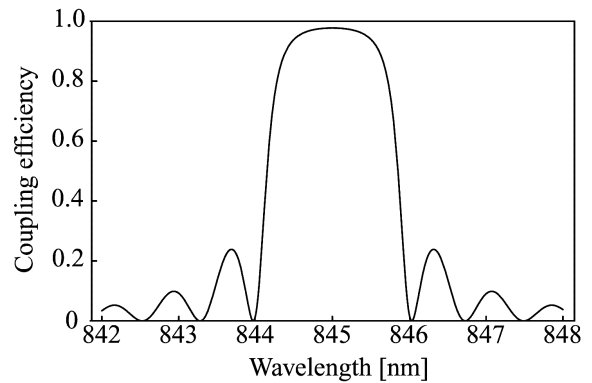


Fig. 3: Calculated wavelength dependence of coupling efficiency

pling efficiency for interaction length of 0.3 mm. A maximum coupling efficiency and full-width at half maximum (FWHM) wavelength-selectivity were calculated to be 97% and 2 nm, respectively. The period Λ of DGM-DBR is given by,

$$\Lambda = \lambda / (N_0^M + N_1^M), \quad (1)$$

where λ is the coupling wavelength, N_0^M and N_1^M are effective refractive indices of TE_0^M and TE_1^M modes, respectively. The effective refractive indices of TE_0^M and TE_1^M modes were calculated to be 1.515 and 1.468, respectively, in the grating area. The grating period was calculated to be 283.27 nm for operating wavelength of 845 nm.

Fabrication

A fabrication process is illustrated in Fig. 4. An election-beam (EB) resist of 0.4- μm thickness was spin-coated on a SiO_2 substrate, and DGM-DBR area of 0.3 mm \times 0.5 mm was patterned by EB direct writing and developing. A Si-N film with thickness of 30 nm and refractive index of 2.01 was deposited by reactive DC sputtering followed by lift-off. An EB resist of 0.3- μm thickness was spin-coated, and DGM-DBR pattern with 283.27-nm period was written by EB direct writing. After developing, the grating pattern was transferred to the Si-N film by reactive ion etching (RIE) using C_3F_8 gas. Figure 5 shows an optical microscopic and a scanning electron microscope (SEM) photographs of the fabricated Si-N grating.

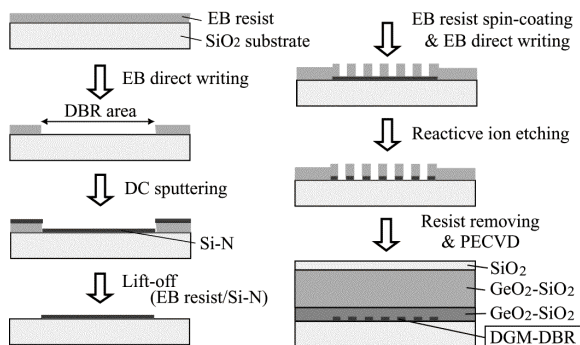


Fig. 4: Fabrication process

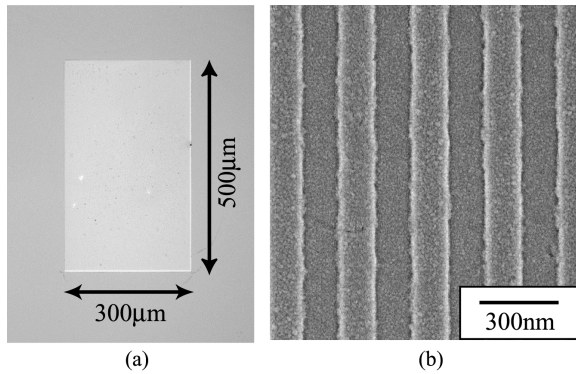


Fig. 5: Microscopic photographs of the fabricated Si-N grating; (a) the whole and (b) part

The grating with line/space ratio of 1:1 could be obtained. A $\text{GeO}_2\text{-SiO}_2$ transmission core layer with refractive index of 1.54 and thickness of $0.8 \mu\text{m}$, a $\text{GeO}_2\text{-SiO}_2$ add/drop core layer with refractive index of 1.47 and thickness of $4.0 \mu\text{m}$, and a SiO_2 covering layer with refractive index of 1.46 and thickness of $0.5 \mu\text{m}$ were sequentially deposited by plasma-enhanced chemical vapor deposition (PECVD) using $\text{Si}(\text{OC}_2\text{H}_5)_4$ and $\text{Ge}(\text{OCH}_3)_4$ as precursors. A grating coupler (GC) of $1.3\text{-}\mu\text{m}$ period, $0.3\text{-}\mu\text{m}$ depth, and $0.5 \text{ mm} \times 0.3 \text{ mm}$ aperture was fabricated by EB direct writing and RIE for exciting TE_1^{M} mode in the waveguide. The reason why the thickness of the covering layer was thinner than the designed value was that the TE_1^{M} mode was excited by the GC with high efficiency. The waveguide ends were fabricated by cleaving after notching backside surface of the substrate. The distance between the GC and DGM-DBR was 10 mm , and the distances between the DGM-DBR and waveguide ends were 20 mm both.

Experimental results

A experimental setup is illustrated in Fig. 6. A tunable laser diode (LD) was used as a light source, and TE_1^{M} mode was excited in the waveguide by the GC. Effective refractive index of TE_1^{M} mode in the GC area was measured to be 1.462 from the incidence angle. Transmitted power as TE_1^{M} mode and reflected power as TE_0^{M} mode were measured at waveguide ends by optical power meter through an objective lens. Figure 7 shows the measured wavelength dependence of the transmitted and reflected power. Open and solid circles show output power of transmitted (TE_1^{M}) and reflected (TE_0^{M}) modes, respectively. A maximum efficiency of 51% was obtained

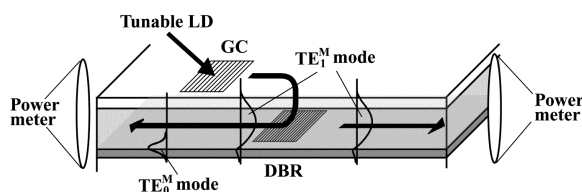


Fig. 6: Experimental setup

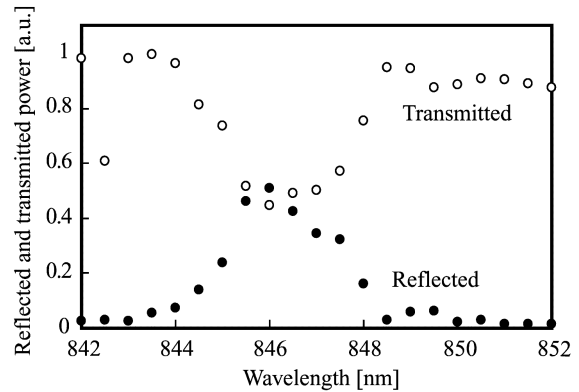


Fig. 7: Wavelength dependence of the fabricated DGM-DBR

at wavelength of 846 nm . FWHM of wavelength selectivity was measured to be 3 nm . The discrepancy between the predicted and measured values in coupling wavelength would be caused primarily by fabrication errors in refractive index and thickness of the fabricated waveguide. The reason for lower reflection efficiency and wider FWHM of wavelength selectivity than the predicted values are currently under study.

Conclusions

We designed and fabricated a DGM-DBR which couples TE_0^{M} and TE_1^{M} modes contra-directionally. Coupling efficiency and wavelength selectivity were theoretically predicted to be 97% and 2 nm , respectively, with interaction length of 0.3 mm at wavelength of 850 nm . Wavelength selectivity of the fabricated DGM-DBR was confirmed experimentally, and the maximum coupling efficiency of 51% was obtained. Experimental work is being continued to improve the coupling efficiency and wavelength selectivity. Application of the DGM-DBR to the proposed add-drop multiplexers is also investigated in order to construct the proposed WDM optical interconnection.

References

- 1 N. Savage, IEEE Spectrum, vol. 39, p. 32, 2002.
- 2 H. Takahara, IEEE J. Select. Topics. Quantum. Electron., vol. 9, p. 443, 2003.
- 3 L. Schares *et al.*, IEEE J. Sel. Top. Quantum Electron., vol. 12, p. 1032, 2006.
- 4 M. Karppinen *et al.*, ECTC, Paper 18-7, 2006.
- 5 H. Schröder *et al.*, ECTC, p. 1053, 2003.
- 6 C. Berger *et al.*, Proc. SPIE, vol. 4942, p. 222, 2003.
- 7 S. Hiramatsu *et al.* : J. Lightwave Technol. vol. 24, p. 927, 2006.
- 8 S. Voigt *et al.*, IEEE Photon. Technol. Lett., vol. 14, p. 1484, 2002.
- 9 M. Chateaufneuf *et al.*, Appl. Opt., vol. 43, p. 463, 2004.
- 10 C. Debaes *et al.*, IEEE J. Sel. Top. Quantum.

- Electron., vol. 9, p. 518, 2003.
- 11 H. Sasaki *et al.*, Appl. Opt., vol. 40, p. 1843, 2001.
 - 12 M. Gruber, Appl. Opt., vol. 43, p. 463, 2004.
 - 13 S. Ura, Proc. SPIE, vol. 4652, p. 86, 2002.
 - 14 K. Kintaka *et al.*, IEEE Photon. Technol. Lett., vol. 16, p. 512, 2004.
 - 15 K. Kintaka *et al.*, Optics Express, vol. 12, p. 3072, 2004.
 - 16 J. Ohmori *et al.*, Jpn. J. Appl. Phys., vol. 44, p. 7987, 2005.
 - 17 S. Ura *et al.*, Appl. Opt., vol. 45, p. 22, 2006.
 - 18 S. Ura *et al.*, Optics Express, vol 14, p. 7057, 2006.
 - 19 A. Horii *et al.*, CLEO-PR, Paper CWK1-4, 2005.
 - 20 K. Kintaka *et al.*, IEEE Photonics Technol. Lett., vol. 18, p. 2299, 2006.
 - 21 K. Kintaka *et al.*, ODF, Paper 7S2-04, 2006.
 - 22 S. Yamaguchi *et al.*, MOC, Paper F-5, 2006.